J Mater Sci: Mater Med (2007) 18:1633–1642
DOI 10.1007/s10856-007-3064-z

Sol-Gel-derived TiO_2–SiO_2 implant coatings for direct tissue attachment. Part II: Evaluation of cell response

Sami Areva · Virpi Ääritalo · Sari Tuusa · Mika Jokinen · Mika Lindén · Timo Peltola

Published online: 5 May 2007

Abstract Silica-releasing sol-gel derived TiO_2–SiO_2 coatings with tailored nanostructure were evaluated in fibroblast and osteoblast cell cultures. The adhesion of both fibroblasts and osteoblasts proceeded within two hours. The highest fibroblast proliferation activities were observed on the TiO_2–SiO_2 (70:30) and (30:70) coatings. However, the cell layer on TiO_2–SiO_2 (30:70) coating was disordered. Prolonged osteoblast activity was observed on the coatings as a function of increased amount of released silica. At day 21 the surfaces were fully covered by the calcified nodules and extracellular matrix except for the coatings TiO_2–SiO_2 (10:90) i.e. having the highest SiO_2 amount. The results suggested that TiO_2–SiO_2 (70:30) was the best for fibroblasts and TiO_2–SiO_2 (30:70) for osteoblasts. The applicability of the sol-gel derived TiO_2 and TiO_2–SiO_2 coatings as an alternative for the calcium phosphate based implant coatings are discussed.

S. Areva (✉) · M. Lindén
Department of Physical Chemistry, Åbo Akademi University, Porthansgatan 3-5, 20500 Turku, Finland
e-mail: sami.areva@utu.fi

S. Areva · S. Tuusa · M. Jokinen · T. Peltola
Turku Centre for Biomaterials, Itäinen Pitkäkatu 4B, 20520 Turku, Finland

V. Ääritalo · M. Jokinen · T. Peltola
Department of Prosthetic Dentistry and Biomaterials Research, Institute of Dentistry, University of Turku, Lemminkäisenkatu 2, 20520 Turku, Finland

Introduction

Titanium has been widely used in medical devices in oral implantology and in orthopedics [1]. Titanium is considered biocompatible and inert material, thus, a fibrous capsule is formed on its surface in vivo and it is not directly attaching to the surrounding tissues. This results in small gaps between the natural bone and implant leading to movement at the implant-tissue interface [2]. To ensure direct contact with bone various methods have been developed. Starting from the surface reactive glasses introduced by Hench et al. [3], and the realization that a formation of a calcium phosphate (CaP) layer on the surface of these glasses is a prerequisite for bone bonding, a variety of CaP ceramic based implant coatings have been applied. Despite their direct attachment to bone, poor adhesion to titanium surface [4, 5] and the inability to produce thin coating layers are the main problems with the implant coatings used today. In addition, the use of plasma spraying is still the only FDA-approved method for the preparation of CaP coatings for clinical applications [2].

An alternative strategy for the ready-made CaP based coatings to ensure direct contact to bone, is to use materials that can initiate CaP formation in situ in the physiological environment. The SiO_2 based bioactive glasses and sol-gel derived TiO_2 coatings belong to this class of materials. In addition, bioinert metals attach directly to bone after they have been made reactive by simple chemical and heat-treatments resulting in TiO_2/TiOH-gel-like structures as recently reviewed by Kokubo et al. [6]. It can be expected that the CaP layer formed in situ is more suitable for the target tissue, since the physiological environment directly influences its formation. This has been explained by the fact that the crystal size of the in situ formed CaP corresponds to that of bone apatite crystals [7]. In addition to

bone bonding, bioactive glasses have been shown to bond to soft tissue as well [8]. Recently, we discovered that sol-gel derived TiO_2 coatings were also able to facilitate direct soft-tissue attachment i.e., without the capsule formation [9]. It was shown that the formation of a thick bone-like CaP layer is not crucial for their integration in soft tissue. Although, all these materials are osteoconductive only SiO_2 based bioactive glasses are osteoinductive [10]. The osteoinductive property of the glasses has been recently connected to the SiO_2 release together with the formed bone-like CaP layer, which is suitable for bone-forming cells [11–13]. It has been shown that certain nanoscale features also influence the cell responses [14–17].

Within the scope of the use of sol-gel derived coatings as implant coatings, we are trying to incorporate the effects that nanoscale topography and released silica have on bone-forming cell activity. In addition, such coatings should also directly attach to soft tissues. In the accompanying Part I of this paper [Ääritalo et al. Submitted], a series of TiO_2–SiO_2 mixed oxide coatings were prepared and extensively characterized. The results showed that we are able to produce silica-releasing coatings with the optimal nanoscale topography for bone growth and contact, respectively. In principle, due to these attractive properties, a good tissue response is expected for these new coatings.

The in vivo bone bonding is commonly modelled in vitro by osteoblast cultures. However, the differences on the origins of the cells make the comparison of the results between different studies difficult [18]. The rat bone marrow cell culture system has gained wide acceptance recently for the in vitro studies of osteogenesis. Bone marrow cells are especially useful models for biomaterials evaluation, because it is a heterogeneous mixture of cells from various lineages, which is close to the in vivo conditions [19, 20]. Because it is well established that a stable soft tissue attachment is of crucial for the long-term implant success rate [21], numerous in vivo studies has been conducted [22]. However, only few in vitro studies have been reported and these have typically been conducted with a simple fibroblast cell culture model. Although, better in vitro models have been created to model the in vivo soft-tissue attachment they have not been extensively used [22]. One reason to use fibroblast cell culture to model soft-tissue conditions is based on in vivo observation that proliferating fibroblasts has a close relation to the materials ability to adhere to soft-tissue [23].

The aim of part II of this paper is to further evaluate the applicability of these coatings using human gingival fibroblasts and rat bone marrow cell cultures to model the soft and hard tissue conditions, respectively. The studied coatings were selected on the basis of their solubility, chemical composition and surface characteristics so that a wide range of different properties would be covered. Thus, TiO_2–SiO_2 coatings having compositions (70:30), (30:70), and (10:90) were selected based on their different silica release properties, which increases as a function of increased SiO_2 amount in the coatings.

Materials and methods

Commercially pure (c.p.) titanium (grade 2) discs were used as the substrate material. All substrates (having dimension of 2×5 cm and thickness of 1 mm) were ground by silicon carbide paper having 500, 800, 1200 grits and washed in acetone and ethanol (5 + 5 min) before the dip coating procedure.

The TiO_2 and TiO_2–SiO_2 sols were prepared to produce the coatings by utilizing the dip-coating procedure. The TiO_2 coating was prepared by dissolving tetraisopropylorthotitanate [TIPT, $Ti((CH_3)_2CHO)_4$] in absolute ethanol and mixed with the solution containing ethyleneglycolmonoethylether ($C_2H_5OCH_2OH$), deionized water, fuming hydrochloric acid (HCl, 37%) and ethanol. The sol was aged 24 h at 0 °C before dipping.

TiO_2–SiO_2 sols were prepared mixing titania and silica sols in different volumetric ratios. The precursor of SiO_2 was TEOS, which is dissolved into ethanol and water at room temperature. The prepared sol was aged at 40 °C for 60 min. For TiO_2, TIPT, ethanol, nitric acid, and water were mixed at room temperature and the obtained titania sol was aged at 40 °C for 30 min. The TiO_2 and SiO_2 sols were mixed in a volumetric ratio so that the desired mole ratios were obtained. Prepared TiO_2–SiO_2 sols were aged at 40 °C and cooled down to the 0 °C for 30 min before dipping process.

The titanium substrates were dipped into the sols withdrawing them at a speed of 0.3 mm/s at ambient atmosphere. After that the substrates were heat-treated in air at 500 °C for 10 min, cooled and washed ultrasonically 5 min in acetone and 5 min in ethanol and dried in air. This cycle was repeated five times. The substrates were cut to 1×1 cm pieces for the cell culture studies. For materials characterization see Part I of this paper for details [Ääritalo et al. Submitted].

Fibroblast isolation and culture

A spontaneously immortalized human gingival fibroblasts (HGF), kindly provided by M.Sc. V. Meretoja, University of Turku, Finland, were cultured in Dulbeccós Modified Eagle Medium (DMEM) supplemented with 10% (v/v) fetal calf serum (FCS) and antibiotics (all from Gibco BRL, Life Technologies, UK) at 37 °C in a humidified 5%

CO_2 atmosphere. Medium was changed three times a week. Trypsinated cell suspension (Trypsin-EDTA 0.25% v/v) from passage 8 was then plated on top of the coated substrates (1×1 cm^2) positioned in 24-well-plates. The cell viability was confirmed by the Trypan-blue exclusion method.

Fibroblast adhesion

Fibroblasts cell suspensions (1 mL; 20,000 cells) were plated on the coated substrates and allowed to adhere for 2, 4 and 6 h. After the adhesion the substrates were fixed for SEM analysis, as described below, to monitor the morphology of the adhered cells.

Fibroblast proliferation

First 100 μL of fibroblasts cell suspension (20,000 cells) were plated on the coated substrates and allowed to adhere for 2.5 h. After adhesion, 900 μL of DMEM was added to the wells and the substrates were cultured for 3, 7 and 14 days. Fibroblast proliferation activity after each time point was determined by the Celltiter 96 non-radioactive cell proliferation assay (CellTiter 96®, Promega, USA) as follows: MTT dye solution was added to the medium and culturing was continued for an additional four hours. Dye reduced by cellular activity was then solubilized and the absorbance at 570 nm was recorded by Shimadzu UV-1601 spectrophotometer. After each time point the substrates were fixed for SEM analysis as described below.

Bone marrow stromal cell culture

Primary bone marrow cells were cultured essentially as described by Maniatopoulos et al. [19]. Rat bone marrow stromal cells were obtained from two male (140–160 g) Sprague-Dawley rats. Femurs were prepared out of connective tissue and washed with 70% ethanol and alpha-MEM (Gibco BRL, Life Technologies B.V. Breda, The Netherlands) with 100 units/mL penicillin/streptomycin (Gibco). The condyles were cut off and bone marrow was flushed out with complete cell culture medium (alpha-MEM, antibiotics supplemented with 15% FCS (Gibco), 50 μg/mL ascorbic acid (Sigma), 10 mM Na-beta-glycerophosphate (Merck, Darmstadt, Germany) and 10 nM dexamethasone (Sigma). The resulting suspension was passed through a 22 G needle and plated cells were cultured in a humidified 5% CO_2 atmosphere at 37 °C. These primary bone marrow derived osteoblastic cells were cultured for 7 days before use. After 7 days of primary culture, the adherent cell population was enzymatically detached (0.25% trypsin/1 mM EDTA; Sigma).

Osteoblast adhesion

Osteoblast cell suspensions (1 mL; 15,000 cells) were plated on the coated substrates and allowed to adhere for 2, 4 and 6 h. After the adhesion the substrates were fixed for SEM analysis, as described below, to monitor the morphology of the adhered cells.

Osteoblast proliferation

First 100 μL of osteoblast cell suspensions (15,000 cells) were plated on the coated substrates and allowed to adhere for 2.5 h at 37 °C in CO_2-incubator. After adhesion, 900 μL of DMEM was added to the wells and the substrates were cultured for 8, 14 and 21 days. Osteoblast proliferation activity after each time point was determined by the Celltiter 96 non-radioactive cell proliferation assay (CellTiter 96®, Promega, USA) as described above for fibroblasts. After each time point the substrates were fixed for SEM analysis as described below.

Osteoblast activity bone nodule formation

At the determined time points, the coatings were washed with PBS and lysed with 50 mM Tris–HCl + 0.1% Triton X-100 in 0.9% NaCl and stored at –70 °C. After thawing the samples were mixed thoroughly and the alkaline phosphatase (ALP) activity was measured from the supernatant. To measure the ALP activity (according Sigma procedure no. 104), 50 μL of alkaline buffer solution and 50 μL of stock substrate solution was added to 30 μL of supernatant (or buffer as blank), and incubated at 37 °C for 15 min. About 870 μL of 0.05 M NaOH was then added to stop the enzymatic reaction and the absorbance readings from three replicate tubes were recorded at 410 nm with Shimadzu UV-1601 spectrophotometer. The measured ALP activity was normalized to the amount of total protein of the same supernatant. Total protein content was measured with Micro BCA protein assay reagent kit (Pierce).

Bone nodule formation

After 14 and 21 days of osteoblast culture the cells were fixed with a double staining method to observe the formation of collagen I fibers. The immunofluorescent labelling of collagen I was done by fixing the PBS washed cells with 2% paraformaldehyde. Then the cells were permeabilized in 0.2% Triton X-100 in PBS. The preparations were incubated with 10% normal goat serum in PBS followed by the incubation with rabbit-anti-rat-collagen type I (1:50 dilution: Cedarlane) antibody in 10% NGS–PBS. Following PBS washing, cells were treated with goat anti-

rabbit FITC-conjugated antibody (1:50 dilution: Zymed) in 10% NGS–PBS. Finally, the cells were mounted with Mounting medium (INOVA) and stored in dark at 4 °C before analysing with a confocal laser scanning microscopy.

Scanning electron microscopy (SEM)

Cellular morphology on the substrates after adhesion and proliferation tests was characterized using SEM-EDS (JEOL JSM-5500). Substrates were washed with phosphate buffered saline (PBS) and cells fixed for 5 min with 2% glutaraldehyde in 100 mM Na-cacodylic acid buffer at pH 7.4 in room temperature. Fixed substrates were then gold coated and stored in a vacuum desiccator before imaging.

Results

Fibroblast adhesion and proliferation

Adhesion times 2, 4 and 6 h were used to study the initial adhesion and growth phases of fibroblast culture on the coatings. On all the coatings fibroblasts adhered well and no significant differences were observed between the coatings. The cells were observed to spread already after 2 h of culture in both TiO_2 and TiO_2–SiO_2 coatings (Fig. 1). After four hours of plating the morphology of the cells are in different phases of adhesion ranging in shape from spherical to mostly flattened. Also, some cells had already obtained a more elongated form (Fig. 2). The cell spreading proceeded at the 6 h time point.

The fibroblast proliferation was slightly enhanced in the SiO_2 containing surfaces compared to the reference TiO_2 coating (Fig. 3). At day 7, the highest proliferation activity was observed on the TiO_2–SiO_2 (30:70) coating. The proliferation activity remained high on all the coatings at day 10, being highest on the TiO_2–SiO_2 (70:30) and (30:70) coatings. Morphologically, the formed cell layers after 3 days of culture were homogeneous and well oriented on the TiO_2 and TiO_2–SiO_2 (70:30) coatings (Fig. 4a and b). Physical contacts between cells had appeared on day 3 on these coatings and the substrate is barely visible under the uniform cell mass. However, the cell layers on TiO_2–SiO_2 (30:70) and TiO_2–SiO_2 (10:90) coatings were disordered (Fig. 4c, d). From day 7 onwards all coatings were fully covered by the cells, but the disordering of the cell layers remained on the TiO_2–SiO_2 (30:70) and TiO_2–SiO_2 (10:90) coatings even after 14 days of culture.

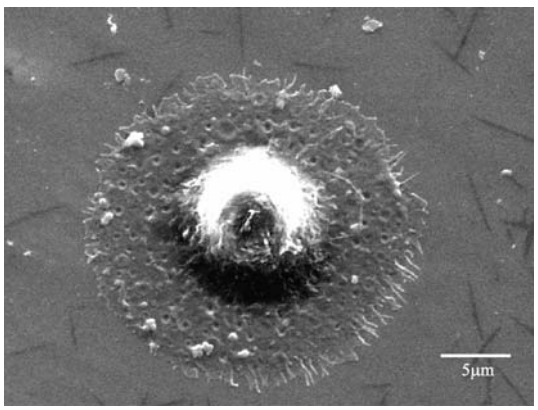

Fig. 1 SEM images of fibroblast cells after 2 h on TiO_2 coating

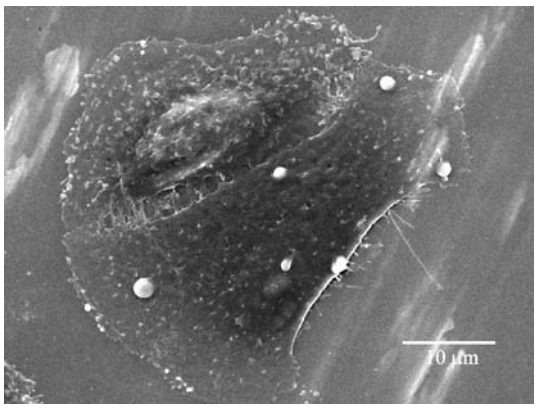

Fig. 2 SEM image of a fibroblast cell after 4 h on TiO_2–SiO_2 (10:90) coatings

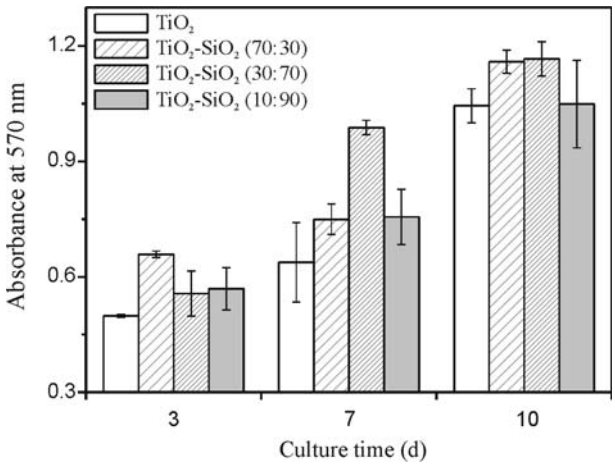

Fig. 3 Proliferation of fibroblasts on sol-gel coatings

Osteoblast adhesion and proliferation

Osteoblasts adhered well on all the coatings and started to spread already after 2 hours of culture. Already after 6 h of culture the cells were mostly flattened on all the coatings (Fig. 5a–d). However, the coatings TiO_2–SiO_2 (30:70)

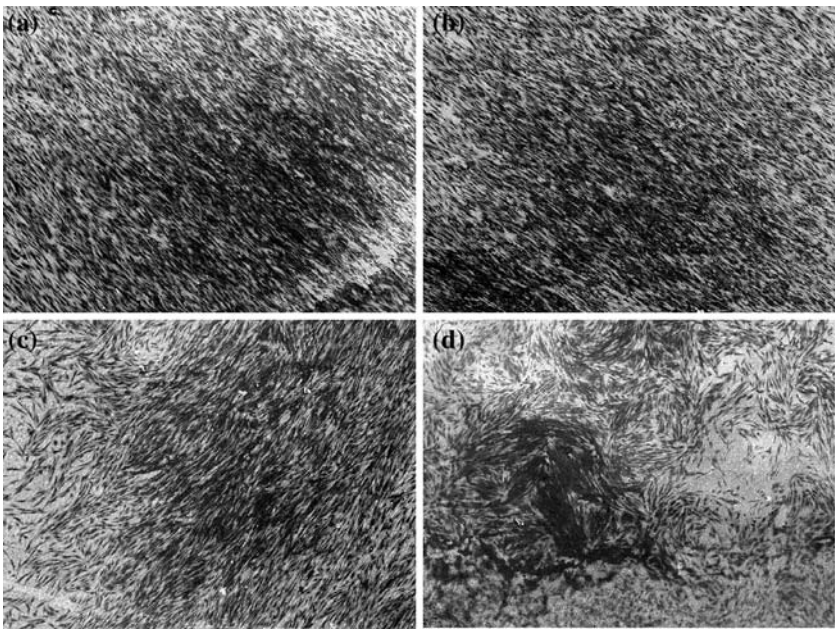

Fig. 4 SEM images of fibroblast cells after 3 days on (**a**) TiO_2, (**b**) TiO_2-SiO_2 (70:30), (**c**) TiO_2–SiO_2 (30:70) and (**d**) TiO_2–SiO_2 (10:90) coatings

(Fig. 5c) and (10:90) (Fig. 5d) showed improved adhesion and cell spreading as compared to the TiO_2–SiO_2 (70:30) (Fig. 5b) and TiO_2 coatings (Fig. 5a). It seems that the flattened cells on the TiO_2–SiO_2 (30:70) coating had attracted a second cell layer to the surface through cell-cell interactions already after 6 h of culture. In addition, on the TiO_2–SiO_2 (10:90) coating at 6 h the cells were more spread as compared to the cells on the other coatings.

The osteoblast growth, as measured by the proliferation activity, peaked at 14 days of culture on all the coatings. No significant differences in proliferation activity were observed between the TiO_2–SiO_2 and reference TiO_2 coatings at days 7 and 14 (Fig. 6). However, significant differences on cell proliferation were observed at day 21. The coatings TiO_2–SiO_2 (30:70) and (10:90) showed still high proliferation activity compared to the TiO_2–SiO_2 (70:30) and TiO_2 coatings.

Osteoblast activity and bone nodule formation

The ALP activity, an early marker for osteoblast differentiation and a measure of the bone forming ability of the

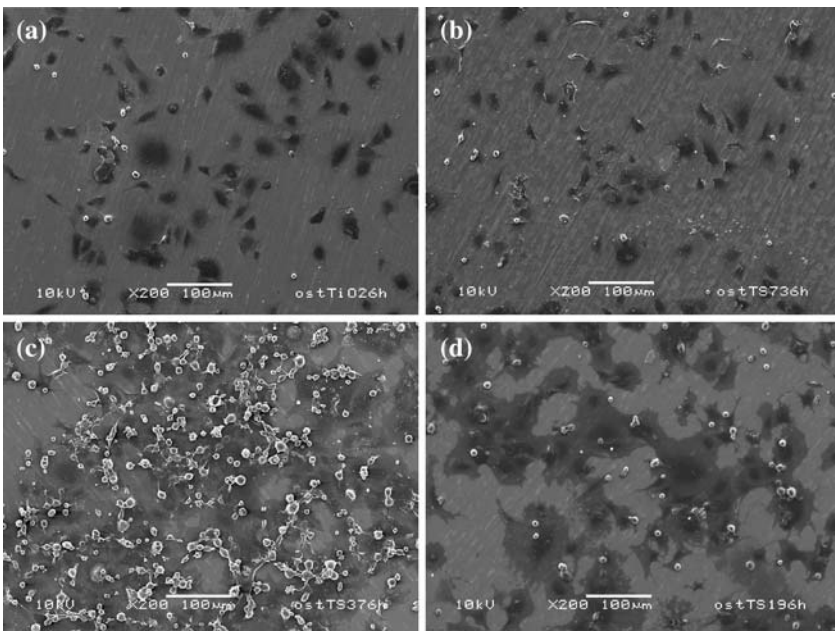

Fig. 5 SEM images of osteoblast cells after 6 h on (**a**) TiO_2, (**b**) TiO_2–SiO_2 (70:30), (**c**) TiO_2–SiO_2 (30:70) and (**d**) TiO_2–SiO_2 (10:90) coatings

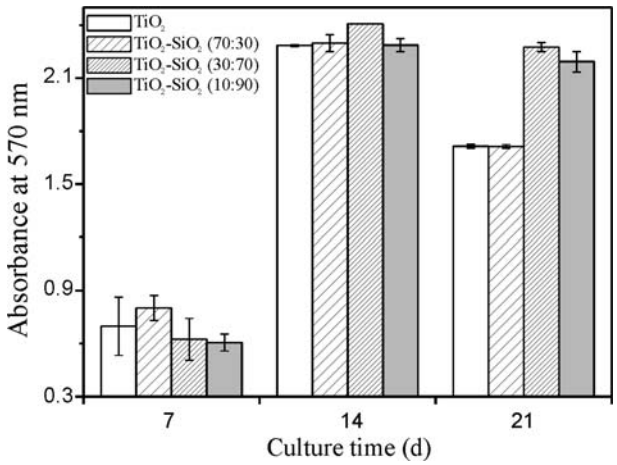

Fig. 6 Proliferation of osteooblasts on sol-gel derived TiO_2 and TiO_2–SiO_2 coatings

osteoblasts, showed significant differences between the materials (Fig. 7). After 7 days of culture TiO_2–SiO_2 (30:70) showed the highest ALP activity. The ALP activity increased on all the coatings from day 7 to day 14, where the highest activities were observed on TiO_2–SiO_2 (30:70) and TiO_2–SiO_2 (70:30) coatings. The lowest ALP activity was observed on the TiO_2–SiO_2 (10:90) coating at both time points. After 21 days of culture the ALP activity decreased significantly on coatings TiO_2 and TiO_2–SiO_2 (70:30). The highest ALP activity at day 21 was found on the TiO_2–SiO_2 coatings (30:70) and (10:90), moreover, the ALP activity on the TiO_2–SiO_2 (10:90) coating remained at the same level as in day 14.

The cell layer after 7 days of culture appeared, based on SEM images, homogeneous and well ordered on all the coatings and no disordering was observed. After 14 days of culture bone nodule formation was observed on

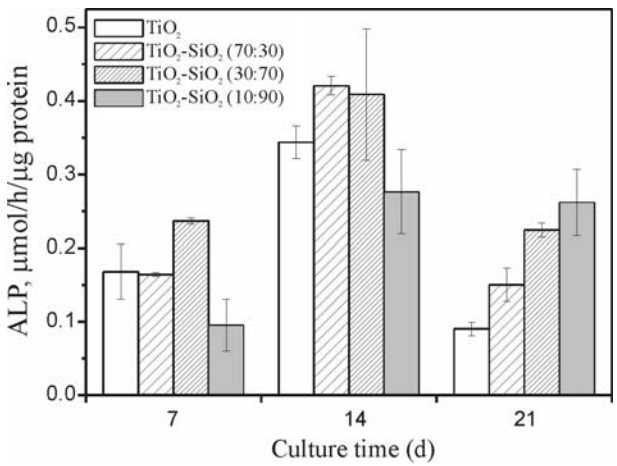

Fig. 7 Activity of alkaline phosphatase on sol-gel derived TiO_2 and TiO_2–SiO_2 coatings

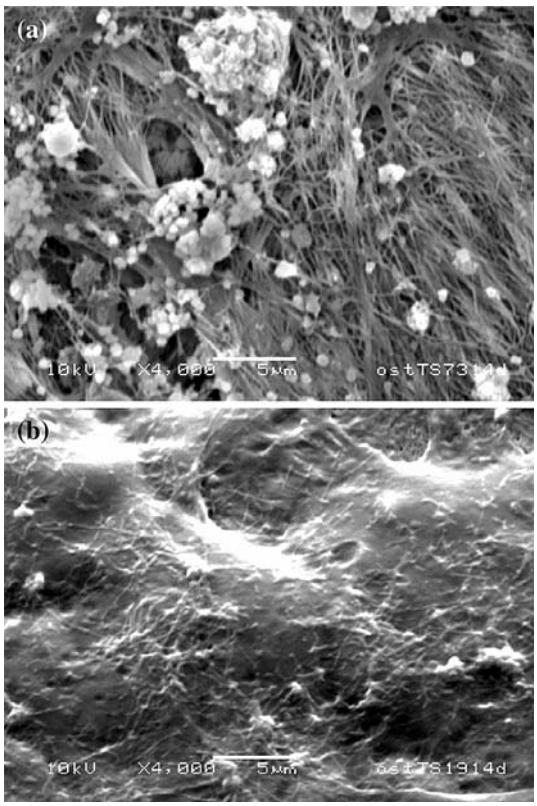

Fig. 8 Representative SEM images of osteoblast cells after 14 days on (**a**) TiO_2–SiO_2 (70:30) and (**b**) TiO_2–SiO_2 (10:90) coatings showing the formation of nodules

coatings TiO_2–SiO_2 (30:70) and TiO_2–SiO_2 (70:30) as well as on the reference TiO_2 coating (Fig. 8). The nodular structures were made by a network of cells exhibiting overlapping and superimposed borders and interconnected processes. Also the cells were producing an extracellular matrix as observed by the formed fibrilar network. The EDS analysis confirmed that the nodular structure was calcified and that the observed particles are precipitated CaP. At day 21 the surfaces were fully covered by the calcified nodules and extracellular matrix. In contrast, osteoblasts cultured in the control well showed only some bone nodule formation only at day 21. By the confocal laser microscopy technique it was observed that the fluorescent stained extracellular matrix consisted of type I collagen and the confocal images collected at different levels showed that the nodules were three dimensional cellular structures within a collagenous extracellular matrix (Fig. 9).

Discussion

The findings of this study makes it possible to extend the results of the Part I of this paper, where silica releasing

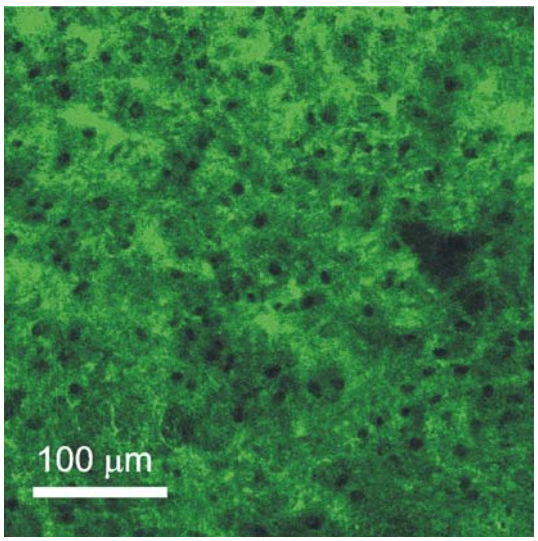

Fig. 9 Representative confocal scanning laser image of the nodule structures on TiO_2–SiO_2 (70:30) coating after 21 days of culture and stained for collagen I

sol-gel derived TiO_2–SiO_2 coatings were successfully prepared. The fibroblast and osteoblast cell behaviours on the TiO_2–SiO_2 coatings were compared to the TiO_2 coating. Both cell types adhered within few hours on these surfaces. The proliferation of fibroblasts was slightly enhanced on the TiO_2–SiO_2 coatings compared to the TiO_2 coating, although significant changes were not observed. However, disorientation was observed in the fibroblasts on coatings containing 70 and 90% SiO_2 after 3 days of culture. These coating exhibited the highest SiO_2 dissolution (see Part I Fig. 8) [Ääritalo et al. Submitted], which might result in surface instability disrupting the growth orientation of the fibroblast cells. In addition, it was observed that the nanoscale surface topography became smoother as the amount of SiO_2 increased in the coatings (see Part I Fig. 5) [Ääritalo et al. Submitted], which might also contribute to the observed growth disorientation of the fibroblasts.

All the coatings showed high osteoblast activity (Fig. 7) and even bone nodule formation after 14 days of culture except the TiO_2–SiO_2 (10:90) coating (Fig. 8). However, both proliferation and ALP activity continued to be high at day 21 of culture for the TiO_2–SiO_2 (30:70) and (10:90) coatings. Thus, the gradual release of SiO_2 from these coatings extends the proliferation and differentiation of the osteoblast on these coatings, which may indicate also enhanced bone-forming ability. Although the SiO_2 levels in solution (approx. 4 and 8 ppm for the TiO_2–SiO_2 (30:70) and (10:90) coatings, respectively) after two weeks of dissolution is lower than the previously demonstrated 20–40 ppm level observed to stimulate osteogenesis [13], the results of this study indicates that the amount of released SiO_2 from the TiO_2–SiO_2 (30:70) and (10:90) coatings is enough to extend osteoblast proliferation and differentiation. This also gives further proof that SiO_2 releasing materials have the potential to stimulate osteoblast even at very low concentrations. Although, the osteoblasts as well as fibroblasts are activated by soluble silica, at least, the fibroblast activation pathway is similar as in the case of toxic response [24]. However, due to the mild toxic effect of soluble SiO_2 the cellular cascade result in enhanced growth factor production, which might explain the observed osteogenesis stimulation by Xynos et al. [11]. Although corresponding phenomenon has been well documented in explaining the mechanism of silicosis [25], further clarifications is needed and are currently conducted in our group.

Although the purpose of this study was to compare the TiO_2–SiO_2 coatings to pure TiO_2 coating, an additional cell culture experiment was done on pure SiO_2 coating, which showed poor cell attachment (Fig. 10) and proliferation (not shown) for both the studied cell types. In part I of this paper, it was shown that the pure SiO_2 coating dissolves almost completely already within two days at the same rate, however, than the TiO_2–SiO_2 (10:90) coating. Thus, the amount of released silica alone does not determine the

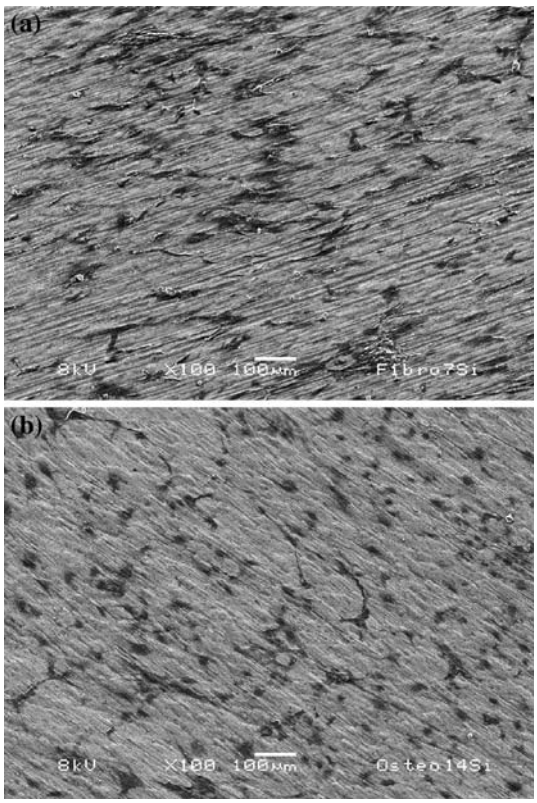

Fig. 10 SEM images of (**a**) fibroblast cells after 7 days and (**b**) osteoblast cells after 14 days on SiO_2 coating

osteoblast or fibroblast activities and the other surface properties must be taken into account.

It is generally considered that the formation of thick bone-like CaP layer on the surface of bioactive material is crucial for its direct attachment to bone. On the other hand, the afore mentioned SiO_2 release from the SiO_2 based bioactive glasses [11–13] and the released Ca from the phosphate glasses [26, 27] has been shown to upregulate gene expression and/or certain protein production of the bone forming cells when cultured in solutions containing the solubility extracts. For example, enhanced collagen type I production has been observed due to silica release [28–30]. Furthermore, Bosetti et al. [28] showed that the collagen I production increased as the amount of SiO_2 increased in the bioactive glasses. In addition, osteblasts showed enhanced adhesion, proliferation and ALP activity on poorly crystalline CaP surfaces compared to crystalline CaP [31, 32] resulting from the enhanced Ca release of the poorly crystalline CaP surfaces. Although the surface instability of bioceramics is considered to be important in osteogenesis induction and bone bonding, it is also thought to cause inflammation of the surrounding tissues, which may lead to failure of the implant [33]. The initial cell adhesion and spreading on the substrate material, which is crucial for cell cycle division, is influenced by the surface instability [34] causing, for example, instability induced lag times in cell adhesion that could explain the inflammation reactions [33]. Although there are many studies on enhanced osteoblast adhesion, proliferation and differentiation on bioactive glasses compared to inactive glasses, cell response inhibition has also been observed on highly unstable bioactive glass surface [35, 36]. To overcome this problem, the surface reactivity and stability has been elegantly combined in the biphasic calcium phosphate bioceramics, where the ratio of stable HA and reactive β-TCP is carefully controlled to get the needed support and reactivity for each implant site as recently reviewed [37, 38].

Similarly, the fibroblasts grown on $CaO–P_2O_5–SiO_2$ based glasses exhibited enhanced fibroblast growth rate only on the glass, which formed a thick CaP layer on its surface, although all the studied glasses released silica [39]. Thus, the formed CaP layer plays an important role also in the fibroblast adhesion and proliferation. Good fibroblast adhesion and proliferation has also been found on phosphate glasses, which form a CaP layer on their surface and the cell response was observed to be enhanced on the more soluble phosphate glass [26]. However, from such a highly unstable surface the fibroblast detached easily and confluent cell layer was not observed [26]. Thus, the essential requirement for a material to show good osteoblast and fibroblast response is the formation of stable support for cell attachment through which the cell activating ions can be leached. These observations are in good agreement with the ones obtained in this study. As stated in Part I of this work [Ääritalo et al. Submitted], the sol-gel derived $TiO_2–SiO_2$ coatings exhibit some of the most suitable surface characteristics for expecting good tissue response. Similarly to glasses exhibiting good cell response the $TiO_2–SiO_2$ coatings are stable enough to facilitate cell attachment, while still releasing SiO_2 from their surfaces. However, these coatings did not form a thick CaP layer on their surface (i.e., a bone-like apatite layer fully covering the surface) after SBF immersion, which is generally considered as an early marker for a material to attach to bone tissue. The coatings were, however, able to nucleate amorphous CaP on their surfaces (Part I). Thus it can be concluded that the formation of a thick CaP layer is not a prerequisite for the observed enhanced osteoblast responses on $TiO_2–SiO_2$. This also highlights the importance of SiO_2 release on cell activation, since the reference TiO_2 coating is able to form a thick CaP layer on its surface.

The adhesion of proteins to solid surfaces also plays an integral role in several key cellular processes. The cell adhesion is mediated by an ill-defined and complex layer of adsorbed proteins. The attachment, spreading and growth of fibroblasts can be influenced by controlled surface chemistries through the adsorbed protein layer [40]. In addition to surface chemistry, the effect of surface nanotopographical features has been found to strongly influence on fibroblast response [17] most likely also through the adsorbed protein layer. Also preadsorption of a protein layer on titanium metal enhances fibroblast adhesion [41] as well as the adsorbed active adhesion sites of proteins, i.e., RGD peptides [42]. Similarly, the importance of protein expression in osteoblast/materials interactions is well established and recently thoroughly reviewed by Anselme [43]. It has been suggested that other proteins than fibronectin e.g. collagen may play a role in osteoblast adhesion to Ti alloys [44], although this is still contradictory [45]. Enhanced vitronectin adsorption has been found on nanoparticles (<100 nm) compared to conventional ceramic particles, which might also explain the observed enhanced osteoblast adhesion of these nanoparticles [14]. However, vitronectin and fibronectin has not been observed on relatively smooth (even on nanoscale) Ti-metal surfaces in osteoblast cultures [46], thus, the observed good cell adhesion on our sol-gel derived coatings might result from the its tailored surface nanostructure (i.e., surfaces are constructed of aggregated 20–50 nm sized particles), which can effectively adsorb these proteins. Although the TiO_2, SiO_2 and $TiO_2–SiO_2$ surfaces are as such biocompatible and stable enough for cell adhesion, the observed nucleation of amorphous CaP has the potential to enhance protein adsorption, which may further enhance cell adhesion and activity [47, 48].

Conclusions

In conclusion, poor implant performance is often caused by the nonintegration of the implant with the surrounding tissue or infection [49]. Furthermore, dental implants, for example, should support at least three types of implant/tissue interfaces, namely, osseointegration, fibro-osseous integration and periodontal connective tissue attachment [50]. Our results show that the TiO_2 and TiO_2–SiO_2 (70:30) coatings showed good cell responses in both fibroblast and osteoblast cultures. Moreover, the TiO_2–SiO_2 (30:70) coating showed prolonged osteoblast activity and calcified nodule formation. However, the results do not provide a clear-cut explanation about the main factor influencing cell response. It is either (i) stimulating effect of released SiO_2 or protein adsorption enhancement either by (ii) a more suitable nanoscale topography or by (iii) coatings ability to nucleate CaP or most likely a combination of them all. In addition, since the observed tissue mineralization (i.e., bone nodule formation in vitro) is suggested to be as cellular mediated (because the cell-free culture showed no mineral formation) these coatings can be used also as templates for synthesis of bone in vitro in tissue engineering.

Acknowledgement M.Sc. Ville Meretoja from the Department of Prosthetic Dentistry and Biomaterials Research, Institute of Dentistry, University of Turku, Finland, is acknowledged for his assistance in cell culture studies. SA would like to thank the Graduate School of Materials Science, Turku, Finland, for financial support. This study was supported by the National Technology Agency, Finland (grant 40725/01).

References

1. P. I. BRÅNEMARK, *J. Prosthet. Dent.* **50** (1983) 399.
2. A. A. CAMPBELL, *Mater. Today* Nov (2003) 26. and the references therein.
3. L. L. HENCH and J. WILSON, In ''*Silicon biochemistry. Ciba Foundation symposium 121*'', edited by D. EVERED and M. O'CONNOR (New York: Wiley, 1986), pp. 231–246.
4. I. M. O. KANGASNIEMI, C. C. P. M. VERHEYEN, E. A. VAN DER VELDEL, and K. DE GROOT, *J Biomed Mater Res* **28** (1994) 563.
5. X. ZHENG, M. HUANG, and C. DING, *Biomaterials* **21** (2000) 841.
6. T. KOKUBO, H. - M. KIM, M. KAWASHITA, and T. NAKAMURA, *J. Mat. Sci: Mater. Med.* **15** (2004) 99.
7. K. KARLSSON, *Ann. Chir. Gyneacol.* **88** (1999) 226.
8. J. WILSON, G. H. PIGOTT, F. J. SCHOEN, and L. L. HENCH, *J. Biomed. Mater. Res.* **15** (1981) 805.
9. S. AREVA, H. PALDAN, T. PELTOLA, T. NÄRHI, M. JOKINEN, and M. LINDÈN, *J. Biomed. Mater. Res.* **70** (2004) 169.
10. L. L. HENCH, *J. Am. Ceram. Soc.* **74** (1991) 1487.
11. I. D. XYNOS, M. V. J. HUKKANEN, J. J. BATTEN, L. D. BUTTERY, and L. L. HENCH, J. M. POLAK, *Calcif. Tissue. Int.* **67** (2000) 321.
12. I. XYNOS, A. EDGAR, L. BUTTERY, L. HENCH, and J. POLAK, *J. Biomed. Mater. Res.* **55** (2001) 151.
13. L. L. HENCH, *Key Eng. Mater.* **192–195** (2000) 575.
14. T. J WEBSTER, C. ERGUN, R. H. DOREMUS, R. W. SIEGEL, and R. BIZIOS, *J. Biomed. Mater. Res.* **51** (2000) 475.
15. T. J. WEBSTER, C. ERGUN, R. H. DOREMUS, R. W. SIEGEL, and R. BIZIOS, *Biomaterials* **22** (2001) 1327.
16. M. J. DALBY, M. O. RICHLE, H. JOHNSTONE, S. AFFROSSMAN, and A. S. G. CURTIS, *Biomaterials* **23** (2002) 2945.
17. M. J. DALBY, M. O. RICHLE, D. S. SUTHERLAND, H. AGHELI, and A. S. G. CURTIS, *J. Biomed. Mater. Res.* **69** (2004) 314.
18. C. SCHMIDT, A. A. IGNATIUS, and L. E. CLAES, *J. Biomed. Mater. Res.* **54** (2001) 209.
19. C. MANIATOPOULOS, J. SODEK, and A. H. MELCHER, *Cell Tissue Res.* **254** (1988) 317.
20. K. NISHIO, M. NEO, H. AKIYAMA, Y. OKADA, T. KOKUBO, and T. NAKAMURA, *J. Biomed. Mater. Res.* **55** (2001) 164.
21. S. KOKA, *Int. J. Prosthodont.* **11** (1998) 421.
22. J. OKSANEN, and M. HERMIA, *J. Periodont.* **73** (2002) 86.
23. Y. KAGEYAMA, Y. YOKOYAMA, K. SUZUKI, Y. HARADA and T. KOKUBO, In *Bioceramics 7*, edited by Ö. H. ANDERSON, R. P. HAPPONEN and A. YLI-URPO (1994) 165.
24. K. - A. KIM, Y. - H. KIM, M. S. SEO, W. K. LEE, S. W. KIM, H. KIM, K. - H. LEE, I. - C. SHIN, J. - S. HAN, H. J. KIM, and Y. LIM, *Tox. Lett.* **135** (2002) 185.
25. R. K. ILER, ''*Chemistry of silica*'' (Wiley, USA, 1979). .
26. M. NAVARRO, M. - P. GINEBRA, and J. A. PLANELL, *J. Biomed. Mater. Res.* **67** (2003) 1009.
27. V. SALIH, K. FRANKS, M. JAMES, G. W. HASTINGS, and J. C. KNOWLES, *J. Mater. Sci.: Mat. Med.* **11** (2000) 615.
28. M. BOSETTI, L. ZANARDI, L. HENCH, and M. CANNAS, *J. Biomed. Mater. Res.* **64** (2003) 189.
29. D. M. REFFITT, N. OGSTON, R. JUDDAOHSINGH, H. F. J. CHEUNG, B. A. J. EVANS, and G. N. HAMPSON, *Bone* **32** (2003) 127.
30. P. VALERIO, M. M. PEREIRA, A. M. GOES, and F. LEITE, *Biomaterials* **25** (2004) 2941.
31. H. - M. KIM, Y. KIM, S. - J. PARK, C. REY, H. M. LEE, M. J. GLIMCHER, J. and S. KO, *Biomaterials* **21** (2000) 1129.
32. J. L. ONG, D. R. VILLARREAL, R. CAVIN, and K. MA, *J. Mater. Sci.: Mater. Med.* **12** (2001) 491.
33. T. SUZUKI, R. OHASHI, Y. YOKOGAWA, K. NISHIKAWA, F. NAGATA, Y. KAWAMOTO, T. KAMEYAMA, and M. TORIYAMA, *J. Biosci. Bioeng.* **87** (1999) 320.
34. S. HUANG, and D. E. INGBER, *Nature Cell. Biol.* **1** (1999) E131.
35. W. C. A. VROUWENVELDER, and C. G. GROOT, K. DE GROOT, *Biomaterials* **13** (1992) 382.
36. E. A. V. EFFAH KUAFMANN, P. DUCHEYNY, and I. M. SHAPIRO, *J Biomed. Mat. Res.* **52** (2000) 783.
37. R. Z. LEGEROS, S. LIN, R. ROHANIZADEH, D. MIJARES, and J. P. LEGEROS, *J. Mater. Mat. Med.* **14** (2003) 201.
38. G. DACULSI, O. LABOUX, O. MALARD, and P. WEISS, *J. Mater. Sci.: Mat. Med.* **14** (2003) 195.
39. G. POLZONETTI, G. IUCCI, A. FRONTINI, G. INFANTE, C. FURLANI, L. AVIGLIANO, D. DEL PRINCIPE, G. PALUMBO, and N. ROSATO, *Biomaterials* **21** (2000) 1531.
40. K. B. MCCLARY, T. UGAROVA, and D. W. GRAINGER, *J. Biomed. Mater. Res.* **50** (2000) 428.
41. K. DERHAMI, J. F. WOLFAARDT, A. WENNERBERG, and P. G. SCOTT, *J. Biomed. Mater. Res.* **52** (2000) 315.
42. K. E. HEALY, *Curr. Opin. Solid State Mater. Sci.* **4** (1999) 381.
43. K. ANSELME, *Biomaterials* **21** (2000) 667.
44. C. - H. KU, D. P. PIOLETTI, M. BROWNE, and P. J. GREGSON, *Biomaterials* **23** (2002) 1447.

45. D. BECKER, U. GEISSLER, U. HEMPEL, S. BIERBAUM, D. SCHARNWEBER, H. WORCH, and K.-W. WENZEL, *J. Biomed. Mater. Res.* **59** (2002) 516.
46. T. MATSUURA, R. HOSOKAWA, K. OKAMOTO, T. KIMOTO, and Y. AKAGAWA, *Biomaterials* **21** (2000) 1121.
47. H. ZENG, K. K. CHITTUR, and W. R. LACEFIELD, *Biomaterials* **20** (1999) 377.
48. K. L. KILPADI, P. - L. CHANG, and S. L. BELLIS, *J. Biomed. Mater. Res.* **57** (2001) 258.
49. A. G. GRISTINA, *Science* **237** (1987) 1588.
50. R. G. CRAIG, and R. Z. LEGEROS, *J. Biomed. Mater. Res.* **47** (1999) 585.